# Structure−Activity Studies of the Regulatory Interaction of the 10 Kilodalton C-Terminal Fragment of Caldesmon with Actin and the Effect of Mutation of Caldesmon Residues 691−696†

Pia A. J. Huber,[‡,§] Yuan Gao,[||] Iain D. C. Fraser,[‡,⊥] O'neal Copeland,[‡] Mohammed EL-Mezgueldi,[‡] David A. Slatter,[||,#] Noeleen E. Keane,[||,#] Steven B. Marston,*[,‡] and Barry A. Levine[||]

*Cardiac Medicine, Imperial College School of Medicine, National Heart and Lung Institute, Dovehouse Street, London SW3 6LY, U.K., and School of Biochemistry, University of Birmingham, Birmingham B15 2TT, U.K.*

*Received July 15, 1997; Revised Manuscript Received December 3, 1997*

ABSTRACT: We have used isotope-edited nuclear magnetic resonance spectroscopy, binding studies, and ATPase activity assays to investigate the interaction with F-actin of the 10 kDa C-terminal 658C fragment of chicken gizzard caldesmon and two site-directed mutants of this fragment. Simultaneous dual-sited contacts with F-actin are observed for the segments of the 658C sequence flanking tryptophan residues 692 and 722. Competition experiments showed that both 658C contacts with actin are displaced by substoichiometric concentrations of the short inhibitory region of troponin-I indicative of different binding sites on actin for these regions of troponin-I and caldesmon. Substitution of caldesmon serine-702 by aspartic acid within the spacer region linking the two actin contacts of 658C led to weaker binding but with retention of equivalent affinity for each interaction site. Differential binding affinity of the two sites was achieved by replacement of the sequence $Glu_{691}$-Trp-Leu-Thr-Lys-$Thr_{696}$ by Pro-Gly-His-Tyr-Asn-Asn. Consistent with these data, the concentration of this Cg1 mutant required to achieve 50% inhibition of actin−tropomyosin-activated myosin ATPase was 4-fold greater than found for the 658C fragment. Although calmodulin binding to Cg1 was observed, calmodulin proved ineffective in relieving the inhibition induced by the binding of this mutant to actin. These results are discussed in light of the actin contacts which are involved in the inhibitory activity possessed by different regions of the C-terminus of caldesmon.

*In vitro* caldesmon binds to actin and inhibits actin-activated myosin ATPase. This inhibition is greatly enhanced by tropomyosin and can be relieved by a $Ca^{2+}$-binding protein such as calmodulin (*1*−*3*). Definition of the interface(s) between actin and caldesmon is thus of specific interest for the analysis of the mechanism of inhibition. On the basis of amino acid sequence and proteolytic digestion, caldesmon may be divided up into four domains (*4, 5*). It is generally agreed that most of the functional properties of caldesmon, including the ability to inhibit the actin−tropomyosin-activated myosin MgATPase activity and the interaction with $Ca^{2+}$-binding proteins releasing this inhibition in the presence of $Ca^{2+}$, are located in the C-terminal domain 4 (some 160 amino acids long) (*6*−*9*). In these respects, the C-terminal domain of caldesmon displays similar biochemical properties to the inhibitory region of striated muscle troponin-I (*10*).

In contrast, the structural basis of regulation by caldesmon and troponin-I appears to differ at the level of their interaction with actin (*11*). The short (11 residue) inhibitory region of troponin-I interacts with the N-terminal residues of actin (*12*), yet modification of these amino acids had only a limited effect on complex formation with caldesmon (*13*). Studies on the properties of fragments of domain 4 representing sequences from N- and C-termini and from the middle of the domain have indicated the presence of several separate regions capable of binding to actin, albeit at reduced affinity, which can participate separately in the inhibition of ATPase activity (*8, 14*−*18*) or in the reduction of relaxed stiffness and active force production in model muscle systems (*19, 20*). The regulatory capacity of these different regions of domain 4 of caldesmon appears to derive from their interaction with distinct segments of actin (*11*).

Studies of the binding to actin of the expressed C-terminal 10 kDa fragment of chicken gizzard caldesmon, 658C [residues 658−756 in the chicken caldesmon sequence (*21*), domain 4b], have indicated that two regions of this fragment, centered on Trp-692 and Trp-722, are involved in actin interaction (*11*). Truncation and deletion mutagenesis of intact caldesmon (*18, 22*) or of domain 4 (*17*) have demonstrated that there are two separate motifs within domain 4b that are related to inhibition of actin−tropomyo-

† This work was supported by the British Heart Foundation, the BBSRC, and the Wellcome Trust. D.A.S. was in receipt of a BBSRC Research Studentship award. We are grateful to BIACORE for the use of a loan instrument.

* To whom correspondence should be addressed. Telephone: +44 171 352 8121 x3307. Fax: +44 171 376 3442. Email: s.marston@ic.ac.uk.

‡ National Heart and Lung Institute.

§ Present address: Division of Medical and Molecular Genetics, UMDS, Guy's Hospital, Lodon SE1 9RT, U.K.

|| University of Birmingham.

⊥ Present address: Vollum Institute L-474, Oregon Health Sciences University, 3181 SW Sam Jackson Park Rd., Portland, OR 97201-3098.

# Present address: School of Biochemistry, University of Bristol.

S0006-2960(97)01727-3 CCC: $15.00 
Published on Web 02/03/1998

sin-activated ATPase. The consensus sequences of these two regions, 690−710 and 713−737, contain the regions around Trp-692 and Trp-722 highlighted by NMR experiments.

To identify the structural basis for these regulatory interactions, we initiated the study by NMR of the recombinant domain 4b of chicken gizzard caldesmon (residues 658−756) expressed in bacteria grown on $^{15}$N-enriched medium. The advantage of NMR in the study of 658C and its actin-binding properties comes from the ability to simultaneously monitor all the amino acids of the polypeptide. We have used isotope-edited 2D and 3D NMR spectroscopic methods to obtain sequence-specific resonance assignments and ($-$N$\underline{\text{H}}-\text{C}_\alpha\underline{\text{H}}$) coupling constant values in combination with site-directed mutagenesis of residues 691−696 and residue 702 as well as biochemical assays to study the functional interaction between actin and the extreme C-terminal region of caldesmon.

## MATERIALS AND METHODS

*Protein Expression and Purification.* The caldesmon mutants 658C, S702D, and Cg1 encompass the chicken gizzard residues 658−756. They were obtained by bacterial expression in the pMW172 plasmid/BL21(DE3) cell system and purified as described by Redwood and Marston (*9*). For further purification of the expressed fragments used in NMR, we added a gel filtration step on Sephadex G50 after ion exchange on S−Sepharose (Pharmacia) and freeze-dried the proteins after extensive dialysis versus $H_2O$. The yield was 15−20 mg of pure protein per liter of expression medium. The production of the mutant plasmid constructs for the expression of 658C and S702D has been described (*9*, *23*). The mutant plasmid for Cg1 was produced by the inverse PCR method (*24*) using the expression plasmid pMW172 encoding 658C (*23*). Two back-to-back primers, 5′-CCTGCTCCAAAACCTTCTGAT-3′ and 5′-CGATTTGTTACCCTCTGG$\underline{\text{G}}$TT$\underline{\text{G}}$TTG$\underline{\text{TAAT}}$GCC$\underline{\text{C}}$T$\underline{\text{GG}}$GTTGATACGACTGGAGAC-3′ (altered nucleotides underlined), were used to change $^{691}$Glu-Trp-Leu-Thr-Lys-Thr$^{696}$ to Pro-Gly-His-Tyr-Asn-Asn. Linear products from the total plasmid PCR were recircularized using T4 DNA ligase and used to transform $Ca^{2+}$-competent JM101 cells. The expression plasmid containing the required mutation, named Cg1, was verified by double-stranded sequencing. The amino acid sequence numbering follows that for chicken gizzard caldesmon (*21*).

$^{15}$N was incorporated into 658C during bacterial expression of the protein by growing the bacteria on a minimal salt medium containing 0.5 g of $^{15}$N-labeled ammonium chloride per liter of medium as $^{15}$N source, described by Muchmore et al. (*25*).

*Protein Extraction and Purification.* Calmodulin was prepared from bovine brain according to the method of Gopalakrishna and Anderson (*26*) and from wheat germ as described by Gao et al. (*27*). Skeletal muscle myosin HMM[1] and actin were prepared by standard methods (*28*, *29*). Tropomyosin was prepared from sheep aorta ether ethanol powder as described by Bailey (*30*) and purified on a hydroxyapatite column (*31*).

Protein concentrations were determined by the method of Lowry et al. (*32*) or by using the calculated extinction coefficients of $\epsilon_{280} = 11\,700\ M^{-1}\ cm^{-1}$ for 658C and S702D and $\epsilon_{280} = 7130\ M^{-1}\ cm^{-1}$ for Cg1.

The troponin-I inhibitory peptide (residues 96−116: Asn$_{96}$-Gln-Lys-Leu-Phe-Asp-Leu-Arg-Gly-Lys-Phe-Lys-Arg-Pro-Pro-Leu-Arg-Arg-Arg-Val-Arg$_{116}$) was prepared and purified by the method previously described (*12*).

*Determination of ATPase Activity.* The effect of 658C and Cg1 on the actin−tropomyosin activation of the myosin ATPase was determined at 25 or 30 °C in 0−20 mM KCl, 5 mM Pipes adjusted to pH 7.0 with KOH solution at 22 °C, 2.5 mM $MgCl_2$, 1 mM DTT (HMM buffer) plus 0.1 mM $CaCl_2$. Protein mixtures were prepared in a final volume of 100 $\mu$L, and the reactions were started by addition of MgATP to 5 mM. After termination of the reactions with 0.5 mL of 10% trichloroacetic acid, the $P_i$ released was measured by the method of Taussky and Schorr (*33*).

*Binding of Caldesmon Fragments to Actin and Actin−Tropomyosin.* The binding of 658C and Cg1 to actin and actin−tropomyosin was determined by cosedimentation. Actin, or actin premixed with smooth muscle tropomyosin to a ratio of 1:0.4 (w/w), was mixed with caldesmon fragments at 25 °C in HMM buffer in a final volume of 100 $\mu$L. An aliquot of 25 $\mu$L was removed, and the remaining 75 $\mu$L was centrifuged at 40000*g* for 60 min. Twenty-five microliters was removed from the supernatant, and the samples before and after sedimentation were separated by gel electrophoresis on 8−18% polyacrylamide, 1% SDS ExcelGels (Pharmacia) and stained with PAGE blue 83 (Merck). The caldesmon bands were estimated by quantitative densitometry using a "Scanmaster3" flat-bed scanner with "Quantity One" software (pdi Inc.). The band area at increasing caldesmon fragment concentrations before sedimentation produced a linear relationship, the equation for which was used to determine the free caldesmon concentration after sedimentation.

*Binding of Calmodulin to 658C and Cg1. (A) Measurements of the Intrinsic Tryptophan Fluorescence of the Caldesmon Mutants.* Fluorescence spectra were recorded on a Perkin-Elmer luminescence spectrometer (LS-5) with excitation at 295 nm in 50 mM NaCl, 10 mM Tris-HCl, pH 7.2, 2.5 mM $MgCl_2$, and 0.1 mM $CaCl_2$ or 0.5 mM EGTA (*34*). Tryptophan fluorescence emission spectra (310−380 nm) were obtained from 5 $\mu$M caldesmon fragments 658C and Cg1. These caldesmon fragments were mixed with increasing concentrations of calmodulin in separate samples. For correction of the emission of $Ca^{2+}$-calmodulin, spectra of $Ca^{2+}$-calmodulin alone were also taken, and the emission intensities at the respective wavelength were subtracted from the fluorescence of the caldesmon−$Ca^{2+}$-calmodulin mixtures.

*(B) Caldesmon Fragment Binding to Calmodulin Using a Biosensor.* Direct binding of 658C or Cg1 to calmodulin in real time was investigated using a BIAcore 2000 system. Wheat germ calmodulin has a single cysteine residue in its N-terminus (Cys-27). This was therefore utilized to im-

[1] Abbreviations: HMM, heavy meromyosin (myosin subfragment); EGTA, ethylene glycol bis($\beta$-aminoethyl ether)-*N*,*N*,*N*′,*N*′-tetraacetic acid; DTT, 1,4-dithio-DL-threitol; PAGE, polyacrylamide gel electrophoresis; HSQC, heteronuclear single quantum correlation; HMQC, heteronuclear multiple quantum correlation; NOESY, nuclear Overhauser effect spectroscopy; TOCSY, total correlation spectroscopy; COSY, correlated spectroscopy; *d*, distance; $^3J_{\text{NH}\alpha}$, coupling constant indicating the $\phi$ backbone torsion angle about each N−$C_\alpha$ bond; MAP (kinase), mitogen-activated protein (kinase); *T*, temperature; K, Kelvin.

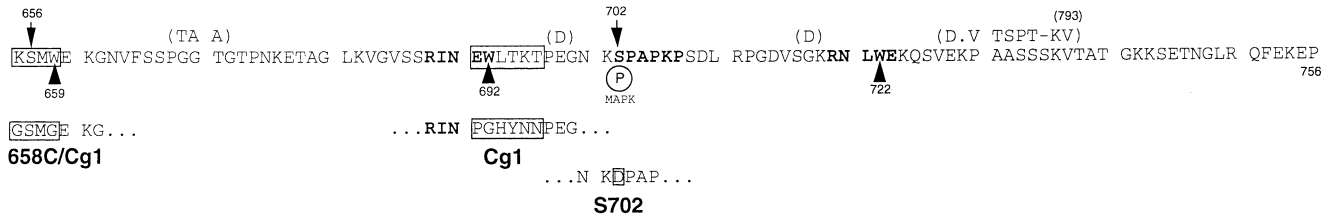


FIGURE 1: Sequence of the 658C and Cg1 fragments of caldesmon. The sequence of chicken gizzard caldesmon domain 4b is numbered according to Bryan et al. (*21*). Amino acids which are different in the human sequence (*58*) are shown in parentheses. The alterations in 658C, S702D, and Cg1 are given in boxes below the original sequence. The caldesmon specific amino acid residues including Trp-692 and Trp-722 as well as the 'spacer' residues are highlighted in boldface (see Results and Discussion). The phosphorylation site, Ser-702, of mitogen-activated protein kinase (MAPK) is indicated (*59*, *60*).

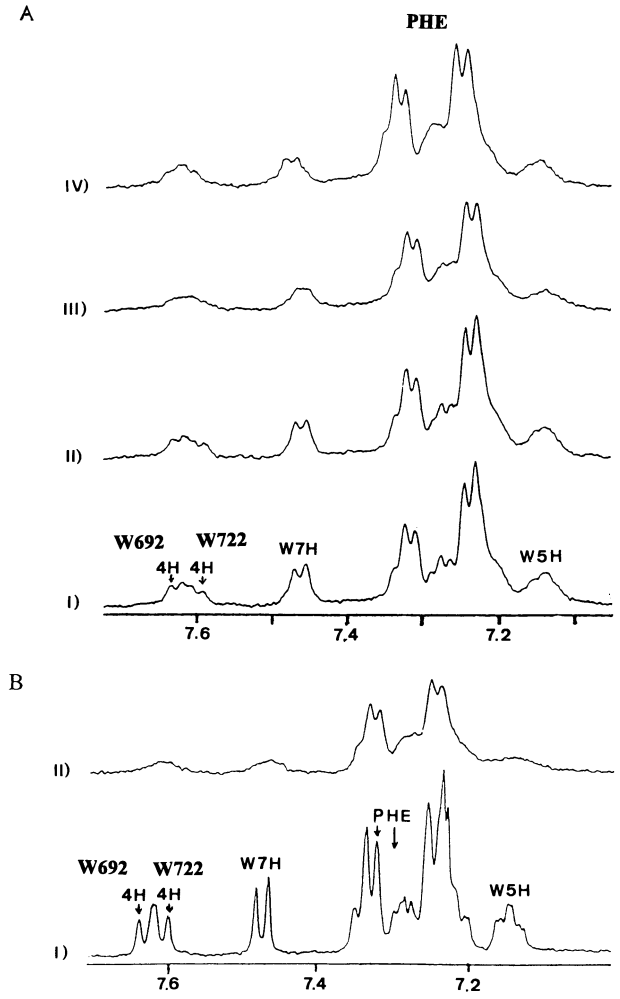


FIGURE 2: Binding of the 10 kDa C-terminal caldesmon fragments, 658C and S702D, to F-actin. (A) $^1$H NMR spectra of 658C at pH 7.2. (i−iii) $T = 285$ K, (iv) $T = 300$ K. (i) 400 $\mu$M 658C, (ii) 658C + 8 $\mu$M actin, (iii and iv) 658C + 16 $\mu$M actin. (B) $^1$H NMR spectra of S702D (400 $\mu$M), pH 7.2, $T = 285$ K: (i) 400 $\mu$M S702D; (ii) addition of 400 $\mu$M actin.

mobilize 1700 resonance units (equivalent to 1.7 ng) of calmodulin (1 mg/mL stock in 10 mM acetate buffer, pH 4.0, 5 mM DTT) on a CM5 sensor chip by the ligand thiol coupling procedure (BIApplications Handbook, Biacore publications, 1993), thereby directing the orientation of all protein molecules on the chip. Two control channels were simultaneously generated: (i) no protein attachment so as to assess adsorption to the chip surface and (ii) calsequestrin so as to assess nonspecific protein interactions. All binding studies were carried out in 20 mM Tris, pH 7.5, 50 mM NaCl, 1 mM $CaCl_2$, 0.05% Tween 20 (running buffer and sample buffer) at a continuous flow rate of 10 mL/min. A series of injections of 658C (or Cg1) were performed over a range of concentrations (100−2000 mg/ml; KINJECT: 120 s injection, 600 s dissociation time). To ensure full dissociation of 658C (or Cg1) from calmodulin, a 60 s application of 100 mM EDTA was performed between each protein injection. The titration data for each binding experiment were analyzed using the BIAevaluation 2.1 package with curve fitting of the dissociation phase for each concentration used in order to derive the dissociation rate constant as for an AB complex dissociation. The protein-free channel was used as a blank. Nonspecific binding of 658C or Cg1 to calsequestrin or to the chip surface was not detected at any time.

*Nuclear Magnetic Resonance (NMR) Spectroscopy.* Solutions of the caldesmon fragments were prepared for the NMR experiments from samples lyophilized from either $^1H_2O$ or $^2H_2O$ at a concentration of 1−3 mM, and spectra were acquired either in 90% $^1H_2O$/10% $^2H_2O$ or in 99.9% $^2H_2O$ using 25 mM deuterated ($d_{11}$) Tris as buffer. No spectral changes suggestive of protein aggregation or denaturation were detected in spectra obtained over the concentration range 0.2−3 mM and pH range of 5−8.

Experiments were carried out on both Varian 600 and Bruker 500 spectrometers with proton frequencies of 599.989 and 500.13 MHz, respectively, and $^{15}$N frequencies of 60.801 and 50.8 MHz, respectively. Spectra were recorded in the pure phase absorption mode by the time-proportional phase incrementation method (*35*). Standard pulse sequences and phase cycling were used for the 2D homonuclear experiments. 2D $^{15}$N−$^1$H HSQC spectra were acquired using the enhanced sensitivity pulsed field gradient methods (*36*, *37*). $^{15}$N decoupling was carried out using the GARP sequence. Solvent suppression for the $^{15}$N−$^1$H spectra was achieved by the use of gradients. Typical data set sizes were 512 increments of 2K complex points with spectral widths of 12 ppm in the $^1$H dimension and 40 ppm in the $^{15}$N dimension. The $^1$H carrier was placed on the water signal, and the $^{15}$N carrier was placed on 98 ppm. Measurements of the $^3J_{NH\alpha}$ coupling constants were obtained using the HMQC-J experiment (*38*) using zero-filling in the $F_1$ dimension to give a final digital resolution of 0.2 Hz per point. Experiments requiring homonuclear Hartman−Hahn spin−lock sequences (3D $^{15}$N−$^1$H TOCSY−HMQC) used a total mixing time of 60 ms (*39*). Heteronuclear 3D experiments were carried out at 600 MHz at 285 K and at pH 5.8 on 3 mM samples. A total of 32 scans per $t_1$ increment were acquired, and NOESY mixing times of 150 and 400 ms used. Spectra were processed using Bruker UXNMR software. Binding titra-

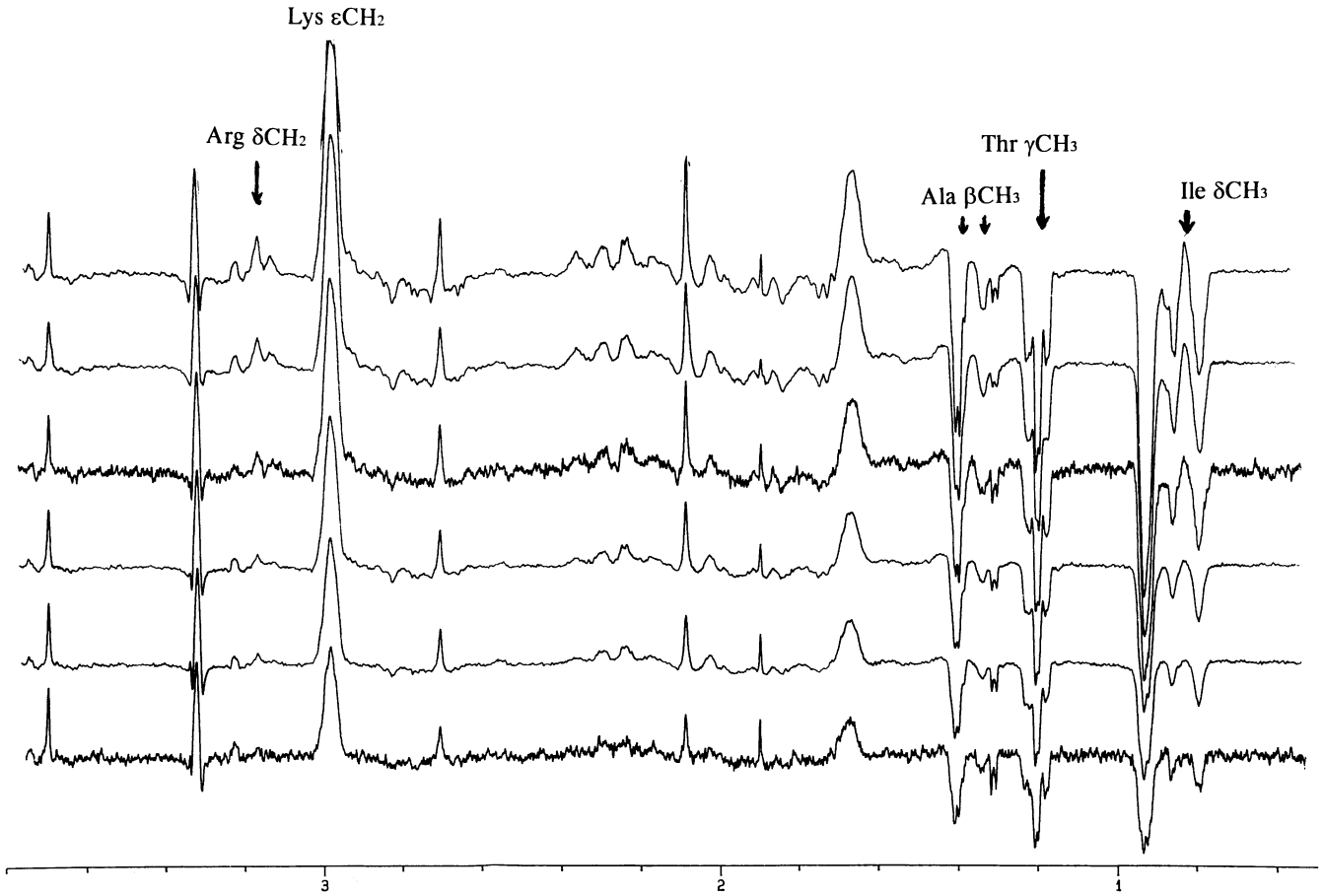


FIGURE 3: Inhibitory troponin-I peptide is readily able to displace 658C from F-actin. Two pulse spin−echo $^1$H NMR spectra (interpulse delay of 60 ms) of 658C−actin upon titration with Tn-I peptide (residues 96−115). Resonance intensity is here indicative of the segmental mobility available to the corresponding groups. Resonance inversion occurs for doublet signals. Bottom trace: Spectrum of 658C (400 $\mu$M, pH 7.2; $T$ = 285 K) after addition of F-actin (160 $\mu$M). Upper traces: addition of troponin-I peptide up to 150 $\mu$M (vs 400 $\mu$M caldesmon fragment).

tions were carried out at 500 MHz by addition of small aliquots of a 10 mg/mL solution of F-actin at a sample pH of 7.2 and at 285 K. Additions were made using a positive displacement pipet to different samples in Eppendorf tubes containing the same volume and concentration of the relevant fragment of caldesmon. Efficient mixing was achieved with a whirlimixer, and the sample then transferred into the NMR sample tube for spectral analysis.

## RESULTS

*Interaction of 658C with Actin Involves Dual-Sited Contacts by the Segments Encompassing Trp-692 and Trp-722.* We have previously observed that both Trp-692 and -722 participate in complex formation of 658C with actin (*11*). To study the nature of these interactions and the relative contributions to binding of the two surrounding regions, titrations with F-actin were carried out using the 658C fragment and a Ser-702 → Asp mutant (S702D) which displays reduced inhibition of the actin−tropomyosin-activated myosin MgATPase activity (*23*); see Figure 1 for primary structures. Addition of F-actin to 658C led to barely detectable changes in the resonance line width and fine structure for the composite aromatic side chain signals of Phe-665 and Phe-752, indicating retention of segmental flexibility at the extremities of the 658C molecule upon actin binding (Figure 2A). In sharp contrast, progressive line broadening of the resonances of both Trp-692 and Trp-722 was observed to occur during titration (Figure 2A). The C4H doublet signals of each of the tryptophan residues were separately resolved and were found to respond in parallel to increasing complex formation. The incremental relaxation induced with increasing actin concentration is indicative of specific complex formation with fast-intermediate chemical exchange on the NMR time scale, a well-documented NMR phenomenon (*40*−*42*). The spectral effect of complex formation at any fraction bound is a sensitive function of the correlation time in the bound complex (*34*). F-Actin is large with a slow tumbling time and a well-organized structure. It is a very effective relaxation sink for those groups in intimate contact. Since the bound line width can therefore be approximated to be infinite by comparison to the free line width, exchange between free and bound forms will result in marked relaxation for the groups in good contact on a time scale shorter than the lifetime of the bound state. The observed signal for the groups of 658C bound to actin (an average over the entire free and bound population) will therefore be broad even at low mole ratios. Hence, the marked effect of substoichiometric actin on the tryptophan signals is a direct indication of close contact between 658C and actin specifically involving residues in the region of 692 and 722. We have observed similar line broadening for the interaction of 658C with spin-labeled $Ca^{2+}$·calmodulin (*34*)

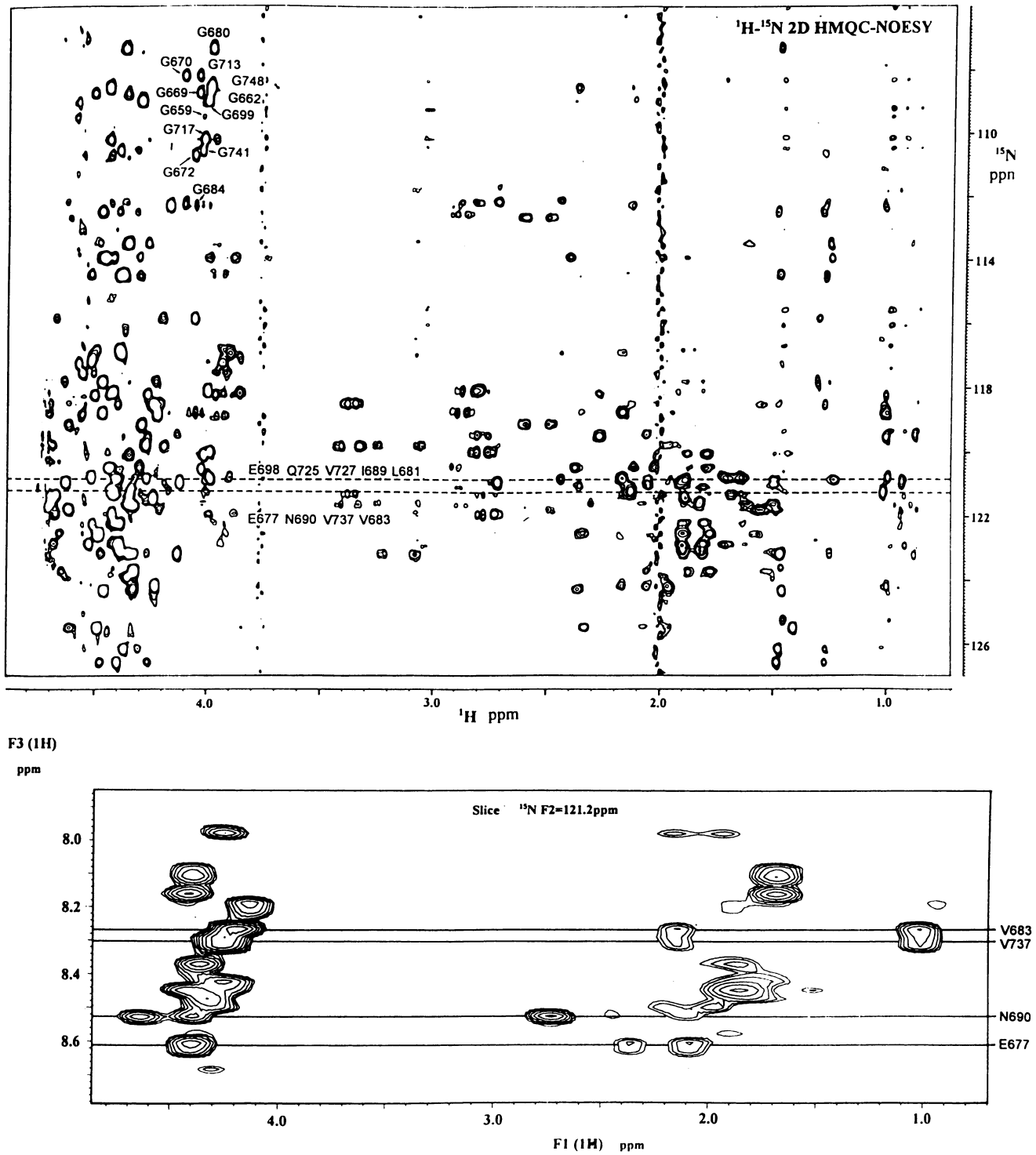


FIGURE 4: Assignment of signals to individual residues in 658C. (A, top) Section of the $^1$H−$^{15}$N 2D HMQC−NOESY spectrum of 658C. (B, bottom) Slice from the $^1$H−$^{15}$N 3D TOCSY−HMQC spectrum of 658C corresponding to the F1−F3 cross section of the 3D spectrum at a $^{15}$N chemical shift of 121.2 ppm. The conventional 2D spectrum of the interacting protons is spread into a third orthogonal frequency dimension. The resolution of Glu-677, Val-683, Asn-690, and Val-737 is apparent. The spectrum was recorded at 600 MHz $^1$H frequency at 297 K and pH 5.5.

and for the interaction of other actin binding peptides such as TnI peptide and the N terminus of myosin LC1 (*12*, *41*).

These observations indicated the dual involvement of the two side chains in the interaction with F-actin. The possibility that the observations could have resulted from equal populations of single-sited attachments involving each tryptophan-containing sequence in turn, rather than a dual-sited mode of binding between 658C and actin, was investigated by monitoring the temperature dependence of the binding reaction. Increasing temperature led to equal effects on the signals of Trp-692 and -722 (Figure 2A), both displaying a significant reduction in line width indicative of equal enhancement of dissociation. Uniform response of the two tryptophan residues was also observed when the S702D mutant was titrated with F-actin (Figure 2B), showing that, although the point mutation led to a reduction in binding

Table 1: $^{1}H$ and $^{15}N$ Resonance Assignments and $^{3}J_{NH\alpha}$ Coupling Constants (Hz) for the 658C Fragment of Caldesmon Obtained at pH 5.6, $T$ = 297 K

| residue | $^{15}N$ | NH | CH$\alpha$ | CH$\beta$ | other | | | $^{3}J_{NH}$ |
|---|---|---|---|---|---|---|---|---|
| Gly659 | 109.5 | 8.57 | 4.03 | | | | | |
| Gly662 | 108.8 | 8.51 | 4.00 | | | | | |
| Gly669 | 108.7 | 8.63 | 4.04 | | | | | |
| Gly670 | 108.2 | 8.39 | 4.11 | | | | | |
| Gly672 | 110.7 | 8.64 | 4.07 | | | | | |
| Gly680 | 107.3 | 8.48 | 3.99 | | | | | |
| Gly684 | 112.3 | 8.65 | 4.06 | | | | | |
| Gly699 | 109.0 | 8.48 | 4.01 | | | | | |
| Gly713 | 108.6 | 8.67 | 4.00 | | | | | |
| Gly717 | 110.2 | 8.52 | 4.02 | | | | | |
| Gly741 | 110.6 | 8.50 | 4.04 | | | | | |
| Gly748 | 108.6 | 8.53 | 3.99 | | | | | |
| Ala679 | 126.2 | 8.46 | 4.37 | 1.48 | | | | 5.49 |
| Ala704 | 125.5 | 8.53 | 4.61 | 1.42 | | | | 5.13 |
| Ala731 | 124.3 | 8.61 | 4.33 | 1.47 | | | | 5.26 |
| Ala732 | 123.1 | 8.54 | 4.40 | 1.48 | | | | 5.13 |
| Ala739 | 126.5 | 8.58 | 4.48 | 1.49 | | | | 7.50 |
| Thr671 | 112.3 | 8.33 | 4.44 | 4.37 | 1.28 $\gamma CH_3$ | | | 8.06 |
| Thr673 | 115.9 | 8.27 | 4.68 | 4.21 | 1.31 $\gamma CH_3$ | | | 7.68 |
| Thr678 | 114.5 | 8.3 | 4.38 | 4.32 | 1.28 $\gamma CH_3$ | | | 8.06 |
| Thr694 | 113.5 | 8.08 | 4.36 | 4.27 | 1.25 $\gamma CH_3$ | | | 8.06 |
| Thr696 | 117.8 | 8.43 | 4.64 | 4.24 | 1.32 $\gamma CH_3$ | | | |
| Thr738 | 118.5 | 8.44 | 4.41 | 4.27 | 1.28 $\gamma CH_3$ | | | 7.93 |
| Thr740 | 112.5 | 8.32 | 4.40 | 4.33 | 1.29 $\gamma CH_3$ | | | 8.19 |
| Thr746 | 113.9 | 8.38 | 4.42 | 4.31 | 1.25 $\gamma CH_3$ | | | 8.19 |
| Val664 | 119.5 | 8.17 | 4.14 | 2.06 | 0.86, 0.99 $\gamma CH_3$ | | | 8.06 |
| Val683 | 121.2 | 8.29 | 4.21 | 2.13 | 1.00, 1.03 $\gamma CH_3$ | | | 8.06 |
| Val685 | 118.8 | 8.19 | 4.23 | 2.21 | 1.00, 1.02 $\gamma CH_3$ | | | 8.06 |
| Val715 | 119.5 | 8.34 | 4.27 | 2.27 | 1.00, 1.03 $\gamma CH_3$ | | | 8.42 |
| Val727 | 120.8 | 8.29 | 4.12 | 2.15 | 0.98 $\gamma CH_3$ | | | 8.79 |
| Val737 | 121.3 | 8.32 | 4.38 | 2.15 | 1.03, 1.01 $\gamma CH_3$ | | | 8.19 |
| Leu681 | 120.9 | 8.12 | 4.39 | 1.68 | 1.63 $\gamma CH$ | 0.93, 0.98 $\delta CH_3$ | | 6.62 |
| Leu693 | 121.7 | 7.97 | 4.35 | 1.61 | 1.56 $\gamma CH$ | 0.89, 0.96 $\delta CH_3$ | | 6.95 |
| Leu710 | 121.3 | 8.16 | 4.24 | 1.68 | 1.68 $\gamma CH$ | 0.92, 0.98 $\delta CH_3$ | | 6.59 |
| Leu721 | 121.8 | 8.34 | 4.21 | 1.54 | 1.47 $\gamma CH$ | 0.86, 0.93 $\delta CH_3$ | | 5.86 |
| Leu749 | 120.8 | 8.18 | 4.43 | 1.71 | 1.64 $\gamma CH$ | 0.98 $\delta CH_3$ | | |
| Ile689 | 120.8 | 8.19 | 4.38 | 1.88 | 1.22, 1.48 $\gamma CH_2$ | 0.92 $\gamma CH_3$ | | 7.32 |
| Asn663 | 118.2 | 8.45 | 4.78 | 2.90, 2.83 | 7.02, 7.69 $NH_2$ | | | |
| Asn675 | 118.8 | 8.67 | 4.71 | 2.89, 2.84 | 7.09, 7.76 $NH_2$ | | | |
| Asn690 | 121.0 | 8.54 | 4.63 | 2.62 | 7.01, 7.69 $NH_2$ | | | |
| Asn700 | 118.1 | 8.44 | 4.78 | 2.82, 2.90 | 7.05, 7.72 $NH_2$ | | | |
| Asn720 | 119.4 | 8.58 | 4.62 | 2.49, 2.60 | 7.01, 7.70 $NH_2$ | | | |
| Asn747 | 120.5 | 8.61 | 4.35 | 2.89, 2.92 | 7.05, 7.76 $NH_2$ | | | 6.95 |
| Asp709 | 121.9 | 8.41 | 4.68 | 2.73, 2.78 | | | | 6.95 |
| Asp714 | 120.0 | 8.24 | 4.69 | 2.74, 2.82 | | | | 6.72 |
| Gln725 | 120.8 | 8.53 | 4.40 | 2.04, 2.15 | 2.44 $\gamma CH_2$ | 6.96, 7.65 $NH_2$ | | |
| Gln751 | 123.9 | 8.60 | 4.62 | 1.98, 2.17 | 2.44 $\gamma CH_2$ | 6.96, 7.61 $NH_2$ | | 5.26 |
| Glu660 | 122.6 | 8.70 | 4.48 | 2.03, 2.18 | 2.37 $\gamma CH_2$ | | | |
| Glu677 | 121.1 | 8.63 | 4.40 | 2.08 | 2.37 $\gamma CH_2$ | | | 6.59 |
| Glu691 | 120.8 | 8.54 | 4.19 | 1.95, 2.17 | 2.37 $\gamma CH_2$ | | | 6.50 |
| Glu698 | 120.5 | 8.68 | 4.78 | 2.03, 2.12 | 2.38 $\gamma CH_2$ | | | 6.59 |
| Glu723 | 121.3 | 8.00 | 4.26 | 1.93 | 2.17 $\gamma CH_2$ | | | 6.59 |
| Glu728 | 124.2 | 8.55 | 4.33 | 1.99 | 2.34 $\gamma CH_2$ | | | |
| Glu753 | 121.7 | 8.40 | 4.28 | 2.12 | 2.34 $\gamma CH_2$ | | | |
| Ser666 | 117.1 | 8.27 | 4.51 | 3.87 | | | | 7.32 |
| Ser686 | 118.8 | 8.62 | 4.56 | 3.96, 4.00 | | | | 6.59 |
| Ser687 | 117.5 | 8.50 | 4.51 | 3.93, 3.97 | | | | 7.19 |
| Ser702 | 117.3 | 8.46 | 4.58 | 3.94, 4.00 | | | | 6.59 |
| Ser708 | 113.9 | 8.43 | 4.42 | 3.89, 4.00 | | | | 6.46 |
| Ser716 | 118.2 | 8.58 | 4.44 | 3.94, 3.97 | | | | 6.59 |
| Ser726 | 116.9 | 8.51 | 4.52 | 3.90 | | | | 6.95 |
| Ser733 | 114.4 | 8.47 | 4.52 | 3.94, 3.98 | | | | 6.59 |
| Arg688 | 122.2 | 8.50 | 4.43 | | | | | 7.93 |
| Arg711 | 123 | 8.64 | 4.68 | 1.82 | 1.73 $\gamma CH_2$ | 3.28 $\delta CH_2$ | 7.44 $\epsilon NH$ | 6.59 |
| Arg719 | 121.3 | 8.44 | 4.25 | 1.84 | 1.77 $\gamma CH_2$ | 3.23 $\delta CH_2$ | 7.32 $\epsilon NH$ | |
| Arg750 | 121.4 | 8.46 | 4.36 | 1.80 | | | | |
| Lys661 | 122.5 | 8.65 | 4.66 | 1.78, 1.88 | 1.57 $\gamma CH_2$ | | | 6.95 |
| Lys695 | 123.1 | 8.31 | 4.47 | 1.82, 1.91 | 1.48 $\gamma CH_2$ | | | 7.32 |
| Lys701 | 121.1 | 8.46 | 4.17 | | | | | |
| Lys706 | 123.7 | 8.56 | 4.65 | 1.78, 1.88 | 1.53 $\gamma CH_2$ | | | 6.95 |
| Lys718 | 120.2 | 8.44 | | | | | | 7.19 |
| Pro668 | | | 4.52 | | | | | |

Table 1 (Continued)

| residue | $^{15}$N | NH | CHα | CH$\beta$ | other | | $^{3}J_{NH}$ |
|---|---|---|---|---|---|---|---|
| Pro674 | | | 4.48 | 1.97, 2.36 | | | |
| Pro697 | | | 4.44 | | | | |
| Pro703 | | | 4.49 | 2.34, 1.97 | | | |
| Pro705 | | | 4.33 | 2.38, 1.98 | | | |
| Pro707 | | | 4.47 | 2.41 | | | |
| Pro712 | | | 4.45 | 2.38, 2.14 | | | |
| Pro730 | | | 4.47 | 2.37, 1.97 | | | |
| Met658 | 121.9 | 8.80 | 4.62 | 2.14, 2.02 | 2.65 $\gamma$CH$_2$ | | |
| Phe665 | 123.2 | 8.48 | 4.75 | 3.22, 3.08 | 2,6H 7.32 | 3,5H 7.39 | 7.32 |
| Phe752 | 119.8 | 8.38 | 4.69 | 3.24, 3.07 | 2,6H 7.33 | 3,5H 7.41 | 7.68 |
| Trp692 | 119.9 | 8.17 | 4.77 | 3.33, 3.40 | 2H 7.32, 4H 7.68 | 5H 7.23, 6H 7.30 | |
| | | | | | | 7H 7.53, NH 10.25 | 7.32 |
| Trp722 | 118.5 | 7.96 | 4.71 | 3.35, 3.38 | 2H 7.31, 4H 7.68 | 5H 7.23, 6H 7.30 | 7.32 |
| | | | | | | 7H 7.53, NH 10.30 | |

affinity as indicated by the higher F-actin concentration required to reach saturation, the nature of the complex still involved dual attachment of both sites to actin.

The residue contexts of Trp-692 and Trp-722 appear to be distinctive of caldesmon as revealed by PROSITE searches based on the sequences -XXRINEW$_{692}$LXX- and -XXRNLW$_{722}$EXX-. The two sequence contexts are substantially less basic than the short inhibitory peptide sequence of troponin-I (amino acid residues 96−115) which has been shown to antagonize 658C binding to actin (*11*). This peptide was therefore used in competition experiments to study whether differential displacement occurred for the two 658C contacts. Titration of the peptide into a 3:1 mole ratio mixture of 658C and F-actin resulted in the progressive reversal of the spectral changes seen for 658C upon actin addition (Figure 3). The concurrent reappearance of the side chain signals of both tryptophan residues indicated the simultaneous displacement of both contacts. This conclusion is supported by the progressive increase in intensity of the triplet $\delta$CH$_3$ signal of the lone isoleucine residue of 658C, Ile-689, which paralleled the behavior of the side chain signals of Trp-692. These observations also pointed to the discrete nature of the 658C−actin contacts since, as seen for Phe-665 and -752, several alanine and threonine CH$_3$ groups retain mobility independent of the overall complex (Figure 3). These residues are distributed throughout the sequence, suggesting that the actin interaction involved fairly restricted segments of the 658C molecule encompassing Trp-692 and -722. To obtain a larger number of sequence-specific spectral assignments and hence more reporter groups for the interaction, 2D and 3D NMR studies of the $^{15}$N-labeled 658C fragment were undertaken.

*NMR Study of the 658C Sequence Indicates Regions of Localized Structure.* Conventional homonuclear $^{1}$H NMR methods for identifying coupled spin systems from scalar (TOCSY) and dipolar (NOESY) connectivities produced limited resonance characterization due partly to substantial signal overlap in the C$_\alpha$H/amide proton fingerprint region of the spectrum. Further, as expected on the grounds of amino acid composition, 24 of the 99 residues showed AMX spin systems for their $\alpha/\beta$ protons (*42*). These spectral features together with the presence of nine proline residues hampered resonance identification by conventional sequential assignment procedures (*42*). The difficulties were largely overcome by making use of the dispersion available in the $^{15}$N chemical shifts of uniformly isotopically enriched 658C. Figure 4A shows a section of the $^{1}$H−$^{15}$N 2D HMQC−NOESY spectrum of 658C where all 12 glycine backbone C$_\alpha$H signals are seen to be resolved in the $^{15}$N dimension. The sequence-specific residue assignments shown are summarized in Table 1. These assignments were readily obtained by 3D $^{15}$N-separated TOCSY and NOESY experiments which enabled the spread of the conventional 2D spectrum of the through-bond/through-space interacting protons into a third (orthogonal) frequency dimension. Figure 4B shows a slice of the $^{1}$H−$^{15}$N 3D TOCSY−HMQC spectrum of 658C where the spectral overlap has been resolved between Val-683 and Val-737 and Asn-690 and Glu-677. The sequence-specific assignments relied on the observation of sequential $d_{NN(i,j+1)}$, $d_{\alpha N(i,j+1)}$, and $d_{\beta N(i,j+1)}$ NOE proximities for the $^{15}$N-labeled protein and also enabled the identification of the previously unassigned aromatic residues. Confirmation of the sequential assignments given in Table 1 was obtained from the observation in *J*-correlation spectra of the characteristic spin systems for the corresponding residues.

To increase the parameter set available from the observed NOEs with a view to localization of relatively structured regions along the protein sequence $^{3}J_{NH\alpha}$ coupling constants indicative of the $\phi$ backbone torsion angle about each N−C$_\alpha$ bond were determined by HMQC-J experiments (Figure 5, Table 1), and qualitative dynamic structural information about different regions of the protein backbone was obtained from the measurement of T1 relaxation times (Figure 5 inset). Inspection of these parameter sets, each reflecting different physical properties of the conformation of the 658C molecule, together with comparison of the $^{1}$H and $^{15}$N chemical shifts with those expected for an unstructured polypeptide (*43*) indicated structural constraints on the segments encompassing the two tryptophan residues. Further, the sequence linking these two segments contains a proline-rich region which was observed to adopt an extended (trans X-Pro) conformation. The 'spacer' properties of the Ser702-Pro-Ala-Pro-Lys-Pro region can be seen from the downfield shift of the -C$_\alpha$H signal of each residue preceding proline [Table 1 and (*44*)] and the strong NOE from the -C$_\alpha$H to the inequivalent C$_\delta$ protons of the neighboring proline ring. Several residues not preceding proline but possessing *J* coupling constant values notably different ($\geq$ 0.7 Hz) from those found in the spectra of denatured proteins (*45*) are observed (e.g., Arg-688, Trp-692, Leu-721, Trp-722, and Val-727), indicative of the more structured nature of the sequences flanking each of the tryptophan residues. This is

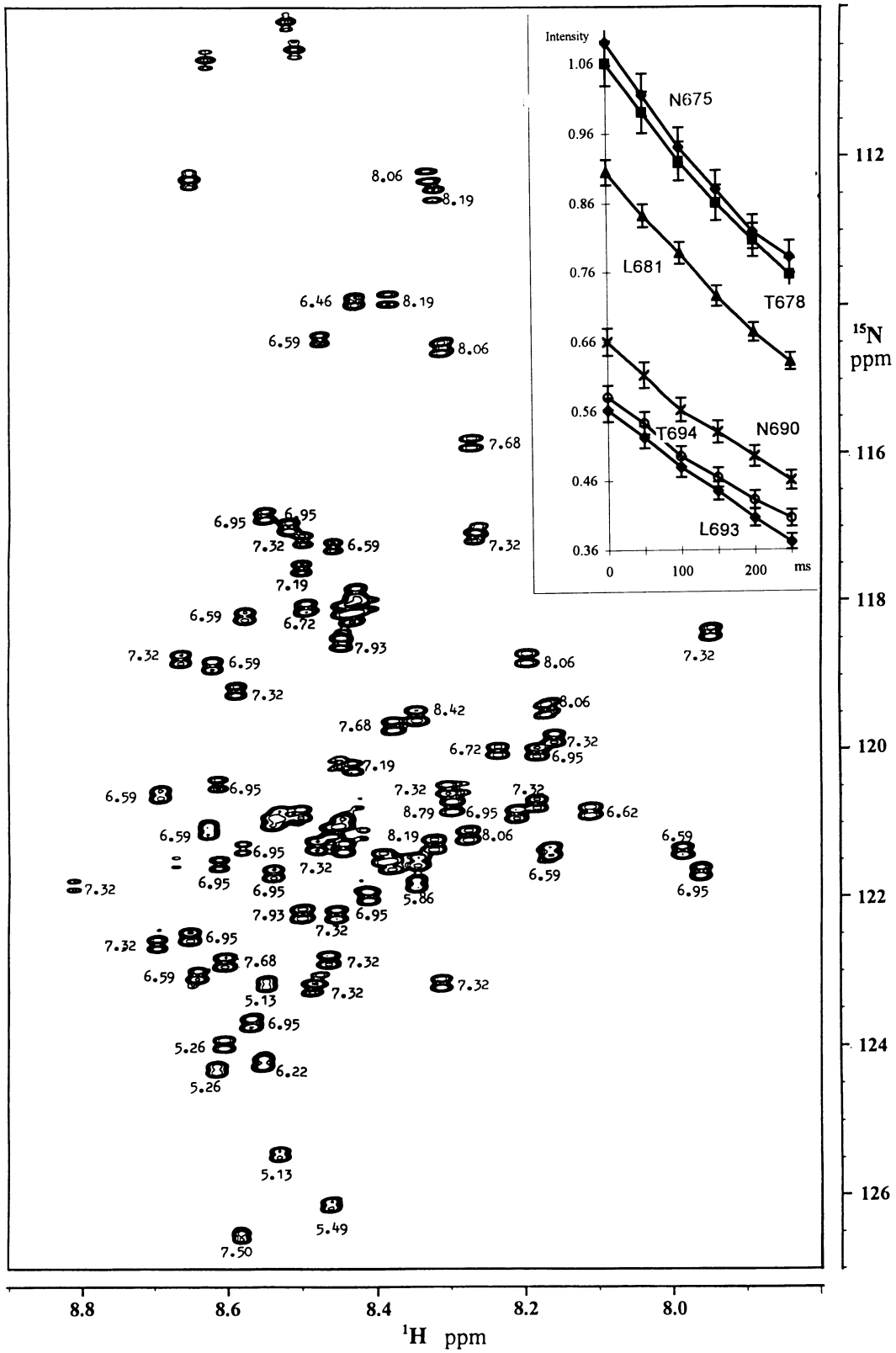


FIGURE 5: Determination of the $^{3}J_{NH\alpha}$ coupling constants which reflect the $\phi$ backbone torsion angle about each N−C$_\alpha$ bond. The $^{1}$H and $^{15}$N HMQC-J spectrum of 658C used for measurement of the NH−C$_\alpha$H coupling constants is shown. The residue assignments are given in Table 1. Inset: Determination of the $^{15}$N T1 relaxation times. Examples of $^{15}$N T1 decay curves for Asn-675, Asn-690, Thr-678, Thr-694, Leu-681, and Leu-693.

also seen in the Figure 5 inset which shows that the backbones of Asn-690, Leu-693, and Thr-694 (surrounding Trp-692) possess different relaxation properties to the same residues (Asn-675, Thr-678, and Leu-681) in the different sequence setting preceding that encompassing Trp-692. A full analysis of these data will be published separately, but it is of interest in view of their dual involvement in actin binding that the two tryptophan-containing regions of domain 4b, fragment 658C, displayed different solvent accessibility. This was judged by the increase in amide proton exchange

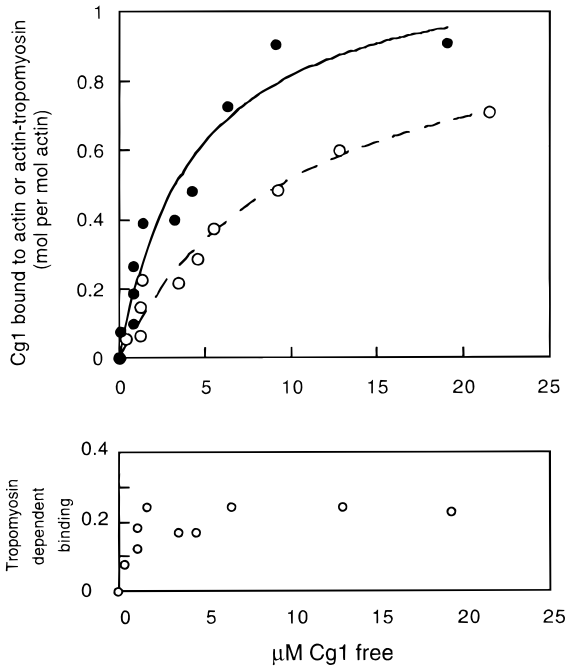


FIGURE 6: Binding of Cg1 to actin or actin−tropomyosin. Conditions: HMM buffer with 10 mM KCl, 25 °C, 12 $\mu$M actin, and, if present, 2.9 $\mu$M tropomyosin. The cosedimentation assay and subsequent analysis are described under Materials and Methods. (○) binding of Cg1 to actin; (●) binding of Cg1 to actin−tropomyosin. The curves are calculated fits to a simple binding equation. Lower panel: Calculated difference between measured Cg1 binding to actin−tropomyosin and the fitted curve for Cg1 binding to actin, showing the high-affinity, low-stoichiometry component of binding which is observed in the presence of tropomyosin. For details of this procedure, see Fraser et al. (*17*).

of specific residues induced by the alteration of the solution pH from 5.8 to 7.2. Since no residue ionization occurred over this pH range, the greater sensitivity of the segment encompassing Trp-722 to base-catalyzed −NH exchange as indicated, for example, by Ser-716, Arg-719, Asn-720, and Leu-721 suggested greater exposure of these residues compared to the sequence adjacent to Trp-692. These considerations influenced our choice of mutagenesis, aiming to affect interaction with actin by alteration of the less solvent-exposed region surrounding Trp-692. We produced a mutant of 658C where we replaced the site around Trp-692, $^{691}$Glu-Trp-Leu-Thr-Lys-Thr$^{696}$ to Pro-Gly-His-Tyr-Asn-Asn replacing the tryptophan residue and changing the local charge of the sequence. The purified fragments, Cg1 and 658C, migrated on SDS−PAGE with the same apparent molecular masses of 10.5 kDa.

*Cg1 Binds to Actin and Actin−Tropomyosin.* The binding of Cg1 to actin or to actin−tropomyosin assessed by sedimentation assay was found to be similar to the binding of 658C in parallel experiments. Figure 6 shows binding curves for Cg1 measured in 10 mM KCl buffer. The binding constants calculated assuming simple binding were $0.1 \times 10^6$ M$^{-1}$ for binding to actin and $0.23 \times 10^6$ M$^{-1}$ for binding to actin−tropomyosin. We previously reported an affinity of $0.06 \times 10^6$ M$^{-1}$ for 658C binding to actin (*9*). It has been demonstrated that the binding of caldesmon and caldesmon peptides such as 658C to actin−tropomyosin may best be accounted for on the basis of two independent binding sites, one with a stoichiometry of 1 per actin and affinity similar to actin binding plus an additional low-stoichiometry (0.07−0.2 per actin), high-affinity tropomyosin-dependent binding component (*9*, *17*, *48*). Our data record was not sufficient to fit to an equation for two classes of binding site; however, when Cg1 binding to actin was subtracted from Cg1 binding to actin−tropomyosin, as described by Fraser et al. (*17*), a high-affinity ($K > 2 \times 10^6$ M$^{-1}$), low-stoichiometry (0.24 per actin) tropomyosin-dependent component of binding was revealed. This compares with $9 \times 10^6$ M$^{-1}$ estimated for the high-affinity binding of 658C at 0 mM KCl using a biphasic fit (*9*).

*$^1$H NMR Reveals That the Mutation of the Sequence Surrounding Trp-692 Reduces Its Affinity for Actin and Results in Differential Dual-Site Interaction.* Addition of actin to the Cg1 mutant showed markedly different apparent affinities of the two actin binding zones of the molecule. While the signals of Trp-722 were significantly perturbed in the initial stages of the titration (Figure 7) in a manner comparable to their response in 658C, the signals of His-693 and Tyr-694 which derive from the mutated region responded only at higher actin concentrations, consistent with an estimated 5−10-fold reduction in the apparent actin binding affinity of this region of the molecule. Further increase in F-actin concentration led to marked broadening of the signals of His-693 and Tyr-694, which showed that, as in the case of 658C, dual sited interaction occurred, leaving other regions of the molecule (e.g., Phe-665 and Phe-752) relatively unaffected by complex formation. Consistent with these observations are our measurements of the inhibitory potency of Cg1.

*Inhibition of the Actin and Actin−Tropomyosin Activation of Myosin ATPase Activity.* The inhibitory potency of 658C and Cg1 on the actin−tropomyosin-activated myosin ATPase was determined in various experimental conditions. At 0 mM KCl/25 °C 3 $\mu$M 658C and 7 $\mu$M Cg1 were needed for 50% inhibition of ATPase activation; at 10 mM KCl, 6 $\mu$M 658C and 30 $\mu$M Cg1 were needed for 50% inhibition (Figure 8A); and at 20 mM KCl/30 °C, 17 $\mu$M 658C and 65 $\mu$M Cg1 were needed for 50% inhibition. Much lower inhibitory activity was observed in the absence of tropomyosin with both caldesmon peptides. Since inhibition is a direct consequence of the caldesmon−actin interaction, we measured actin binding and inhibition of actin−tropomyosin activation of HMM ATPase activity in parallel experiments (Figure 8B). While 50% inhibition resulted when 0.1 mol of 658C was bound per mole of actin, the amount of bound Cg1 needed for the same inhibition level was some 3−4× higher. These results clearly show that the mutation of the six amino acid residues causes a decrease of the cooperativity of the ATPase inhibitory effect of the C-terminus of caldesmon when bound to actin−tropomyosin.

*Both Caldesmon Fragments Bind to $Ca^{2+}$-Calmodulin.* As previously shown for 658C, we observed that Cg1 was able to bind calmodulin in a $Ca^{2+}$-dependent manner. Using fluorescence spectroscopy, we observed a distinct blue shift of the maximum of the intrinsic tryptophan fluorescence of the caldesmon fragments upon complex formation of both 658C and Cg1 with calmodulin, in the presence but not in the absence of $Ca^{2+}$(Figure 9A), in accordance with previous observations of complex formation of caldesmon with $Ca^{2+}$-calmodulin (*34*, *46*, *47*). The concentration of calmodulin required to give half-maximal fluorescence blue shift was greater for Cg1 than for 658C indicating weaker binding of

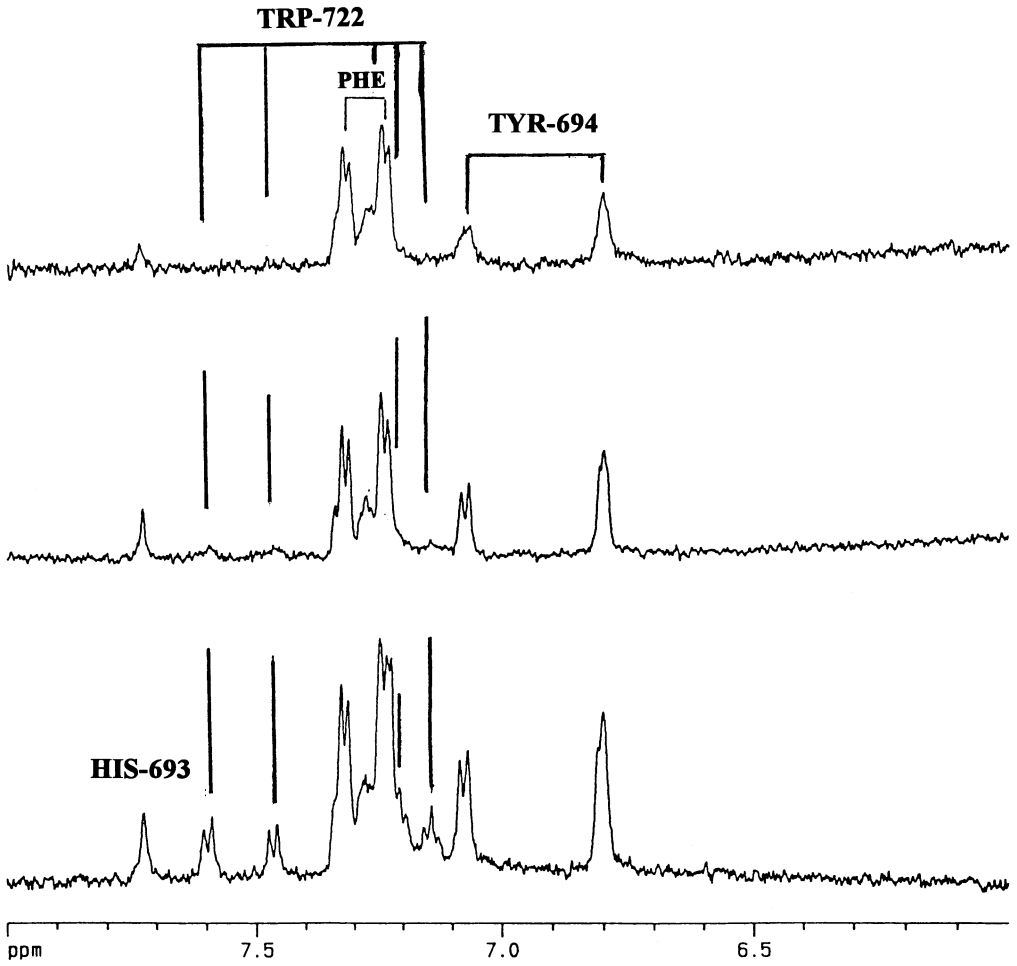


FIGURE 7: NMR spectra of the titration of Cg1 with F-actin. The aromatic region is shown to illustrate the differential effects found for Trp-722, His-693, and Tyr-694. Bottom trace: proton NMR spectrum of Cg1 (400 $\mu$M; pH 7.2; 297 K). Upper traces: spectrum after addition of actin at (middle) 10 $\mu$M and (top) 110 $\mu$M.

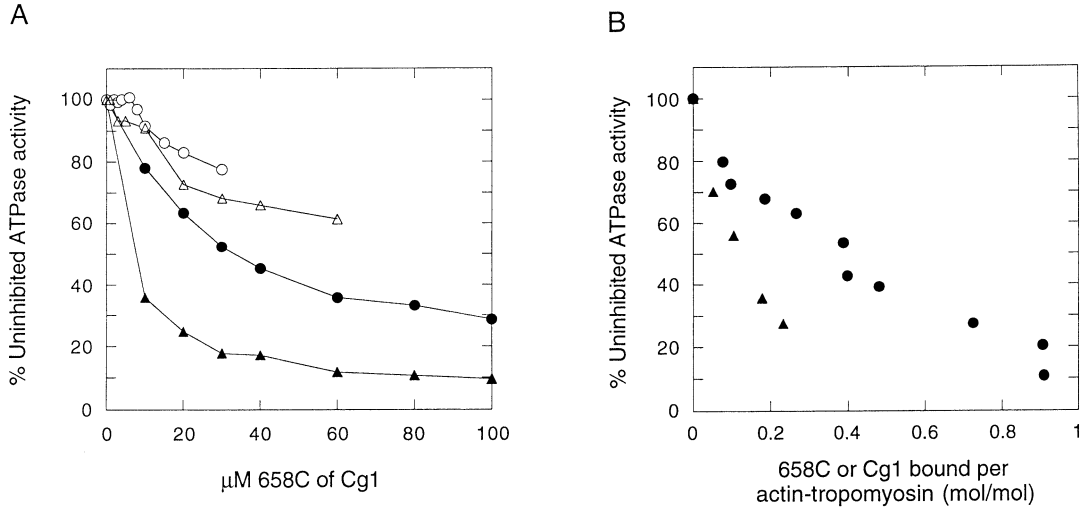


FIGURE 8: Inhibition of the actin and actin−tropomyosin-activated myosin ATPase by Cg1 and by 658C. Panel A conditions: HMM buffer with 10 mM KCl/25 °C (in the presence of tropomyosin, closed symbols) or with 0 mM KCl/25 °C (in the absence of tropomyosin, open symbols), 1 $\mu$M skeletal muscle HMM, 12 $\mu$M actin, 4 $\mu$M tropomyosin (if present), and 0−100 $\mu$M caldesmon fragment. Cg1: (○, ●). 658C: (△, ▲). The assay is described under Materials and Methods. Uninhibited ATPase (=100% ATPase) was 2.6 and 7.5 $s^{-1}$ in the absence and presence of tropomyosin, respectively. Panel B: Inhibition of actin−tropomyosin activation in relation to actin binding. Conditions: HMM buffer with 0 mM KCl and 0.1 mM $CaCl_2$, 25 °C, 1 $\mu$M skeletal muscle HMM, 12 $\mu$M actin, 4 $\mu$M tropomyosin. Cg1: (●). 658C: (▲). Uninhibited ATPase was 1.8 $s^{-1}$ (=100% ATPase).

Cg1. The interaction of Cg1 with calmodulin was also indicated by a biosensor-based binding assay when solutions of different concentrations of both Cg1 and 658C were injected past calmodulin-bound and control surfaces. The quantitative difference in binding detected during this wash-on phase was confirmed by the relative ease with which each

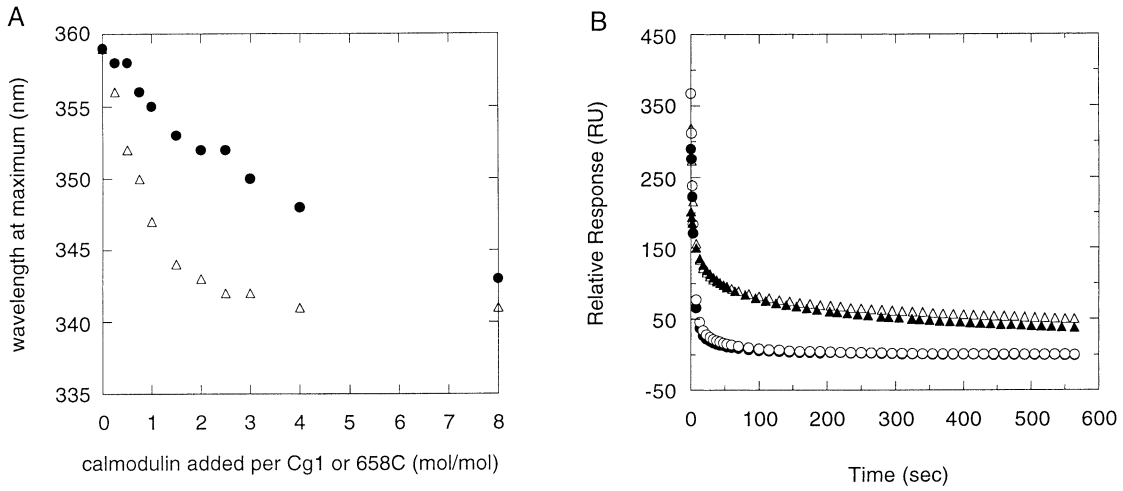


FIGURE 9: Binding of Cg1 or 658C to $Ca^{2+}$-calmodulin. (A) Measurement of the tryptophan fluorescence emission of caldesmon fragments Cg1 and 658C. The wavelength of maximum tryptophan fluorescence of 658C or Cg1 was measured (excitation at 295 nm) upon titration with calmodulin as described under Materials and Methods. Cg1: (●). 658C: (△). Apparent dissociation constants derived from these titrations were 4 ± 1 $\mu$M and 15 ± 4 $\mu$M for 658C and Cg1, respectively. (B) Biosensor: Overlay of the dissociation curves of 658C (▲, △) and Cg1 (●, ○) during the wash-off phase following injection onto the calmodulin-coated chip surface. A series of injections of 658C and Cg1 were performed over the range of concentrations 100−2000 mg/mL; 1000 (●, ▲) and 1500 mg/mL (△, ○) shown for each. Before each injection, the level of associated protein was reduced to base line by a 10 mL injection of 100mM EDTA. Curves have been normalized by subtraction of the reference, blank channel. The wild-type 658C can be seen to dissociate more slowly than Cg1. The dissociation rate constants ($s^{-1}$) derived by curve fitting of the dissociation phase time courses were 0.065 ± 0.002 ($n$ = 3) and 0.113 ± 0.003 ($n$ = 3) for 658C and Cg1, respectively.

caldesmon fragment dissociated from calmodulin during the wash-off phase following injection (Figure 9B), indicating that the affinity of calmodulin for 658C was greater than its affinity for the Cg1 mutant.

We also examined the ability of $Ca^{2+}$·calmodulin to reverse inhibition of actin−tropomyosin due to 658C and Cg1. Measurements were made in 20 mM KCl at 25 °C; 20 $\mu$M 658C inhibited actin−tropomyosin activation by 50%, and the inhibition was reversed by adding $Ca^{2+}$·calmodulin (50% reversal at 5 $\mu$M) as previously observed (*34*, *48*). In contrast, 60 $\mu$M Cg1 was needed for 50% inhibition, and $Ca^{2+}$·calmodulin had no effect upon inhibition, even at 200 $\mu$M, the highest concentration tested.

## DISCUSSION

It has been established that the whole of the inhibitory property of caldesmon is contained within the C-terminal approximately 160−170 amino acid residues, corresponding to domain 4, and that the C-terminal 99 amino acids (domain 4b) retain tropomyosin-dependent, $Ca^{2+}$·calmodulin-regulated inhibition of actomyosin ATPase activity, albeit with a lower affinity for actin (*6*, *7*, *8*, *9*, *18*, *49*). Our results show that the interaction of caldesmon domain 4b with F-actin involves docking of two noncontiguous segments which flank Trp-692 and Trp-722 (Figure 2). Our data also indicate that the stretch of the polypeptide chain ($Ser_{702}$−Pro-Ala-Pro-Lys-$Pro_{707}$) linking these two actin contacts adopts an extended, relatively rigid configuration able to act as both spacer and swivel joint. Although our results indicate that the contact sites on actin are disparate, they do not distinguish between interaction of both sites on a single actin monomer surface from dual-sited attachment spanning two monomers.

Ser-702 at the N-terminus of the spacer segment has been identified as a MAP kinase phosphorylation site (*50*). Introduction of a negatively charged residue in the linker segment of the S702D mutant led to lower affinity for actin but did not alter the dual-sited nature of the protein contacts formed (Figure 2B). In sharp contrast, differential affinity of these two contacts resulted from the alteration of residues 691−696 in the Cg1 mutant (Figure 7). This suggested the separate ability of each site to interact with F-actin. It is thus most likely that the weaker affinity for the two sites observed in S702D derives from a slower on-rate and/or faster dissociation kinetics. Ser-702 indeed occurs within a motif comprising charged residues, Lys695-x-x-Asp/Glu-x-x-Lys701-x-x-x-Lys-x-x-Asp709, which is unique to caldesmon. The observed effect of negative charges at position 702 indicates that this characteristic charge distribution of the spacer motif may be a contributing factor in the dual-sited association between F-actin and the C-terminal 658C fragment of caldesmon.

The reduced propensity of residues 691−696 to take on a helical structure was one reason behind the introduction of proline at residue 691 of the Cg1 mutant, aiming to probe any difference in conformation when docked to F-actin and to calmodulin. Despite the marked difference between 658C and Cg1 in the nature of the side chains of residues 691−696, it is notable that this mutated site was capable of interacting with the actin surface, albeit with lower affinity (Figures 6 and 7). The contrasting inability of calmodulin to compete for Cg1 in the presence of actin can therefore be rationalized in terms of the intrinsic structural bias of the mutated residues of Cg1, a conclusion supported by the observation that the short segment comprising residues 687−695 became helical when bound to calmodulin (*51*). The ability retained by Cg1 to form dual-sited contacts with F-actin indicated that complex formation with F-actin involving residues 691−696 was not reliant upon the properties of their side chains alone and suggested that this region of caldesmon is likely to adopt a more open conformation when bound to F-actin, possibly looped rather than helical.

Our results are also consistent with the deletion mutagenesis studies of caldesmon (*22*), which indicate that excision of residues 690−717 and 718−735 led to reduced actin binding and lower inhibitory potency, and with deletion analysis of domain 4 (*17*), which indicated that the sequences 690−710 and 713−737 were essential for inhibition. Our data shed further light on the different locales of actin that underlie the inhibitory ability of the C-terminal domain 4 of caldesmon. Despite the occurrence of lysine residues throughout the sequence of the 658C fragment comprising domain 4b (13% by residue composition), no cross-linking by EDC to actin has been reported, unlike that observed between the short inhibitory region of troponin-I and the acidic residues at the N-terminus of actin (*52*). Rather, interaction of this region on domain 1 of actin with domain 4a of caldesmon has been indicated by cross-linking (*53*) and demonstrated by NMR (*11*). It thus appears that the ability of 658C (and Cg1) to inhibit actomyosin ATPase in a manner potentiated by tropomyosin utilizes sites other than at actin's N-terminus. This conclusion is supported by our observation of the ready displacement of both actin contacts on each of the caldesmon fragments by the 21 residue troponin-I inhibitory peptide. Similar displacement by the binding of the troponin-I peptide to actin's N-terminal was found for the myosin light chain 1 which interacts at the C-terminal residues on subdomain 1 of actin (*54*). Since the topology of the C-terminal region of caldesmon involves proximity of the segments flanking Trp-692 and Trp-722 to Cys-580 (*11*), a residue that can be cross-linked to Cys-374 of actin (*55*), our observations suggest that the contact(s) and inhibitory ability of 658C entail(s) interaction of caldesmon domain 4b at the C-terminus of actin. This is consistent with three-dimensional reconstructions of the complex of F-actin with caldesmon domain 4 (the caldesmon fragment, 606C) demonstrating the presence of extra mass at the C-terminus of actin in the complex (*56*). The interaction of the C-terminal domain 4 of caldesmon at a number of sites on the surface of actin [this study and (*11*, *57*)] raises the possibility of a graded inhibitory response modulated by the prevailing concentration of calmodulin or other relevant calcium-binding proteins.

## REFERENCES


1. Sobue, K., Takahashi, K., and Wakabayashi, I. (1985) *Biochem. Biophys. Res. Commun. 132*, 645−651.
2. Dabrowska, R., Goch, A., Galazkiewicz, B., and Osinska, H. (1985) *Biochim. Biophys. Acta 842*, 70−75.
3. Ngai, P. K., and Walsh, M. P. (1985) *Biochem. J. 230*, 695−707.
4. Wang, C.-L. A., Wang, L.-W. C., Xu, S., Lu, R. C., Saavedra-Alanis, V., and Bryan, J. (1991) *J. Biol. Chem. 266*, 9166−9172.
5. Marston, S. B., and Redwood, C. S. (1991) *Biochem. J. 279*, 1−16.
6. Szpacenko, A., and Dabrowska, R. (1986) *FEBS Lett. 202*, 182−186.
7. Riseman, V. M., Lynch, W. P., Nefsky, B., and Bretscher, A. (1989) *J. Biol. Chem. 264*, 2869−2875.
8. Bartegi, A., Fattoum, A., Derancourt, J., and Kassab, R. (1990) *J. Biol. Chem. 265*, 15231−15238.
9. Redwood, C. S., and Marston, S. B. (1993) *J. Biol. Chem. 268*, 10969−10976.
10. Marston, S. B., Fraser, I. D. C., and Huber, P. A. J. (1994) *J. Biol. Chem. 269*, 32104−32109.
11. Mornet, D., Bonet-Kerrache, A., Strasburg, G. M., Patchell, V. B., Perry, S. V., Huber, P. A. J., Marston, S. B., Slatter, D. A., Evans, J. S., and Levine, B. A. (1995) *Biochemistry 34*, 1893−1901.
12. Levine, B. A., Moir, A. J. G., and Perry, S. V. (1988) *Eur. J. Biochem. 172*, 389−397.
13. Crosbie, R. H., Miller, C., Chalovich, J., Rubenstein, P. A., and Reisler, E. (1994) *Biochemistry 33*, 3210−3216.
14. Chalovich, J. M., Bryan, J., Benson, C. E., and Velaz, L. (1992) *J. Biol. Chem. 267*, 16644−16650.
15. EL-Mezgueldi, M., Derancourt, J., Callas, B., Kassab, R., and Fattoum, A. (1994) *J. Biol. Chem. 269*, 12824−12832.
16. EL-Mezgueldi, M., Copeland, O., Fraser, I. D. C., Marston, S. B., and Huber, P. A. J. (1997) *Biophys. J. 71*, A332 (Abstract).
17. Fraser, I. D. C., Copeland, O., Wu, B., and Marston, S. B. (1997) *Biochemistry 36*, 5483−5492.
18. Wang, Z., Horiuchi, K. Y., and Chacko, S. (1996) *J. Biol. Chem. 271*, 2234−2242.
19. Malmqvist, U., Arner, A., Makuch, R., and Dabrowska, R. (1996) *Pflügers Arch. 432*, 241−247.
20. Heubach, J. F., Hartwell, R., Ledwon, M., Kraft, T., Brenner, B., and Chalovich, J. (1997) *Biophys. J. 72*, 1287−1924.
21. Bryan, J., Imai, M., Lee, R., Moore, P., Cook, R. G., and Lin, W. G. (1989) *J. Biol. Chem. 264*, 13873−13879.
22. Wang, Z., and Chacko, S. (1996) *J. Biol. Chem. 271*, 25707−25714.
23. Redwood, C. S., Marston, S. B., and Gusev, N. B. (1993) *FEBS Lett. 327*, 85−89.
24. Clackson, T., Gussow, D., and Jones, P. T. (1993) in *PCR: A practical approach* (McPherson, M. I., Quirke, P., and Taylor, I. R., Eds.) pp 187−214, IRL Press, Oxford, U.K.
25. Muchmore, D. C., McIntosh, L. P., Russel, C. B., Anderson, E., and Dahlquist, F. W. (1989) *Methods Enzymol. 177*, 44−55.
26. Gopalakrishna, R., and Anderson, W. B. (1982) *Biochem. Biophys. Res. Commun. 104*, 830−836.
27. Gao, Y., Levine, B. A., Mornet, D., Slatter, D. A., and Strasburg, G. M. (1992) *Biochim. Biophys. Acta 1160*, 22−34.
28. Margossian, S. S., and Lowey, S. (1982) *Methods Enzymol. 85*, 55−71.
29. Straub, F. B. (1942) *Stud. Inst. Med. Chem., Univ,. Szeged 2*, 3−16.
30. Bailey, K. (1948) *Biochem. J. 43*, 271−273.
31. Eisenberg, E., and Kielley, W. W. (1974) *J. Biol. Chem. 249*, 4742−4748.
32. Lowry, O. H., Rosebrough, N. J., Farr, A. L., and Randall, R. J. (1951) *J. Biol. Chem. 193*, 265−275.
33. Taussky, H. H., and Schorr, E. (1953) *J. Biol. Chem. 202*, 675−685.
34. Huber, P. A. J., EL-Mezgueldi, M., Grabarek, Z., Slatter, D. A., Levine, B. A., and Marston, S. B. (1996) *Biochem. J. 316*, 413−420.
35. Marion, D., and Wüthrich, K. (1983) *Biochem. Biophys. Res. Commun. 113*, 967−974.
36. Bax, A., Ikura, M., Kay, L. E., Torchia, D. A., and Tschudin, R. (1990) *J. Magn. Reson. 86*, 304−318.
37. Kay, L. E., Brooks, B., Sparks, S. W., Torchia, D. A., and Bax, A. (1989) *J. Am. Chem. Soc. 111*, 5488−5490.
38. Kay, L. E., and Bax, A. (1990) *J. Magn. Reson. 86*, 110−126.
39. Marion, D., Driscoll, P. C., Kay, L. E., Wingfield, P. T., Bax, A., Gronenborn, A. M., and Clore, G. M. (1989) *Biochemistry 28*, 6150−6156.
40. Lian, L.-Y., and Roberts, G. C. K. (1993) in *NMR of Macromolecules: a practical approach* (Roberts, G. C. K., Ed.) pp 153−182, IRL Press, Oxford U.K.
41. Levine, B. A., Moir, A. J. G., Trayer, I. P., and Williams, R. J. P. (1990) in *Molecular Mechanisms of Muscle Contraction* (Squire, J., Ed.) pp 171−209, MacMillan Press, New York.
42. Wüthrich, K. (1986) in *NMR of proteins and nucleic acids*, Wiley, New York.

43. Wishart, D. S., Bigham, C. G., Abildgaard, F., Dyson, H. J., Oldfield, E., Markley, J. L., and Sykes, B. D. (1995) *J. Biomol. NMR 6*, 135−140.
44. Bhandari, D. G., Levine, B. A., Trayer, I. P., and Yeadon, M. E. (1986) *Eur. J. Biochem. 160*, 349−356.
45. Smith, L. J., Bolin, K. A., Schwalbe, H., MacArthur, M. W., Thornton, J. M., and Dobson, C. M. (1996) *J. Mol. Biol. 255*, 494−506.
46. Shirinsky, V. P., Bushueva, T. L., and Frolova, S. I. (1988) *Biochem. J. 255*, 203−208.
47. Medvedeva, M. V., Kolobova, E. A., Huber, P. A. J., Fraser, I. D. C., Marston, S. B., and Gusev, N. B. (1997) *Biochem. J. 324*, 255−262.
48. Smith, C. W., Pritchard, K., and Marston, S. B. (1987) *J. Biol. Chem. 262*, 116−122.
49. Hayashi, K., Fujio, Y., Kato, I., and Sobue, K. (1991) *J. Biol. Chem. 266*, 355−361.
50. Adam, L. P., and Hathaway, D. R. (1993) *FEBS Lett. 322*, 56−60.
51. Zhou, N., Yuan, T., Mak, A. S., and Vogel, H. J. (1997) *Biochemistry 36*, 2817−2825.
52. Grabarek, Z., and Gergely, J. (1987) *Biophys. J. 51*, 331a.
53. Bartegi, A., Fattoum, A., and Kassab, R. (1990) *J. Biol. Chem. 265*, 2231−2237.
54. Grand, R. J. A., Levine, B. A., and Perry, S. V. (1982) *Biochem. J. 203*, 61−68.
55. Graceffa, P., and Jancso., A. (1991) *J. Biol. Chem. 266*, 20305−20310.
56. Hodgkinson, J. L., Marston, S. B., Craig, R., Vibert, P., and Lehman, W. (1997) *Biophys. J. 72*, 2398−2404.
57. Levine, B. A., Moir, A. J. G., Audemard, E., Mornet, D., Patchell, V. B., and Perry, S. V. (1990) *Eur. J. Biochem. 193*, 687−696.
58. Humphrey, M. B., Herrera-Sosa, H., Gonzalez, G., Lee, R., and Bryan, J. (1992) *Gene 112*, 197−205.
59. Childs, T. J., Watson, M. H., Sanghera, J. S., Campbell, D. L., Pelech, S. L., and Mak, A. S. (1992) *J. Biol. Chem. 267*, 22853−22859.
60. Adam, L. P., Gapinski, C., and Hathaway, D. R. (1992) *FEBS Lett. 302*, 223−226.

BI971727B